

# High-Sensitivity Bolometers from Self-Oriented Single-Walled Carbon Nanotube Composites

Gustavo Vera-Reveles,<sup>†,‡</sup> Trevor J. Simmons,<sup>†,‡,§</sup> Mariela Bravo-Sánchez,<sup>†</sup> M. A. Vidal,<sup>†</sup> Hugo Navarro-Contreras,<sup>†</sup> and Francisco J. González\*,<sup>†</sup>

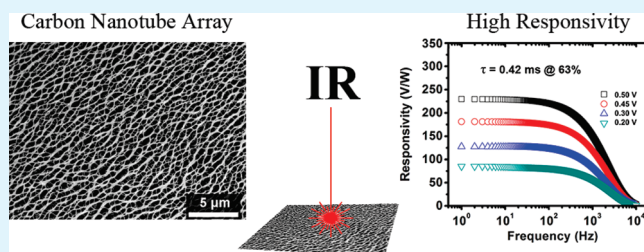
<sup>†</sup>Coordinación para la Innovación y la Aplicación de la Ciencia y la Tecnología, Universidad Autónoma de San Luis Potosí, San Luis Potosí 78000, México

<sup>‡</sup>Department of Chemistry & Chemical Biology, Rensselaer Polytechnic Institute, 110 Eighth Street, Troy, New York 12180, United States

 Supporting Information

**ABSTRACT:** In this work, films of horizontally aligned single-walled carbon nanotubes were thermally and electrically characterized in order to determine the bolometric performance. An average thermal time constant of  $\tau = 420 \mu\text{s}$  along with a temperature coefficient of resistance of  $\text{TCR} = -2.94\% \text{ K}^{-1}$  were obtained. The maximum voltage responsivity and detectivity obtained were  $R_V = 230 \text{ V/W}$  and  $D^* = 1.22 \times 10^8 \text{ cm Hz}^{1/2}/\text{W}$ , respectively. These values are higher than the maximum voltage responsivity (150 V/W) and maximum temperature coefficient of resistance (1.0% K<sup>-1</sup>) previously reported for carbon nanotube films at room temperature. The maximum detectivity was obtained at a frequency of operation of 1.25 kHz.

**KEYWORDS:** bolometers, carbon nanotubes, infrared detectors, noise, detectivity



## 1. INTRODUCTION

In recent years, great effort has been devoted to the development of infrared (IR) thermal imaging devices because of their numerous military, medical, and commercial applications.<sup>1</sup> Single-walled carbon nanotubes (SWNTs) are quasi-one-dimensional structures with a remarkable band structure which results in unique electrical, mechanical, and optical characteristics.<sup>2,3</sup> Along with their remarkable electronic properties, carbon nanotubes (CNTs) combine large surface area, chemical stability, high strength and significant elastic properties, which make them appropriate candidates for applications such as supercapacitors,<sup>4</sup> batteries,<sup>5</sup> heat exchange systems,<sup>6</sup> and actuators.<sup>7</sup> Optical and thermoelectric characterization of thin films of SWNTs has shown IR absorption coefficients higher than 70% for 100 nm thick films,<sup>8</sup> temperature coefficient of resistances (TCRs) that ranged from 1 to 2.5% K<sup>-1</sup> for SWNT suspended in vacuum<sup>8</sup> over a temperature range of 330–100 K and voltage responsivities ( $R_V$ ) around 150 V/W.<sup>9</sup>

In this work, densely packed and highly aligned films of horizontally aligned single-walled carbon nanotubes (SWNTs) in a polymer/surfactant matrix were thermally and electrically characterized in order to determine their bolometric performance. These materials showed exceptional bolometric properties, and in many respects can outperform previously reported carbon nanotube bolometers, approaching the performance of commercially available metal oxide bolometers.

## 2. EXPERIMENTAL METHODS

Purified SWNTs grown using a high-pressure carbon monoxide method (HiPCO) were purchased from Carbon Nanotechnologies Inc. (now Unidym Inc.) Lot No. P0279, and were mixed with deionized water and sodium dodecylbenzenesulfonate (SDBS, Aldrich). The solute and solvent were thoroughly combined by sonic agitation provided by a bath-type sonicator for 30 min, after which a polymer surfactant, polyvinylpyrrolidone (PVP-10, Aldrich), was then added and the solution was sonicated for an additional 5 min.

The obtained carbon nanotube solution, or “ink”, was then deposited to yield horizontally aligned arrays of SWNTs. This was achieved by placing several drops of the SWNT-containing ink on a [100] silicon wafer substrate and then drying at room temperature for several hours.<sup>10,11</sup> Two vertical silver stripes (10 mm long, 1.2 mm wide, and 7.6 mm apart) were deposited atop the horizontally aligned SWNTs using a conductive silver paint, and were used as electrical contacts for bolometric characterization.

The resistance and temperature coefficient of resistance (TCR) was measured in real time using two Fluke 289 digital multimeters with data-logging capabilities to measure voltage and temperature while heating the SWNT film with a Peltier thermoelectric device. The TCR was calculated from relationship 1

$$\text{TCR} = \frac{1}{R} \frac{dR}{dT} \quad (1)$$

**Received:** June 1, 2011

**Accepted:** July 12, 2011

**Published:** July 12, 2011

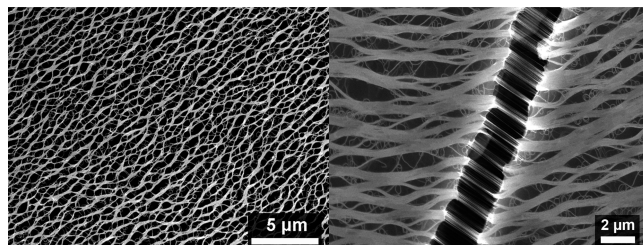


**Figure 1.** Scanning electron micrograph of horizontally aligned SWNTs forming dense networks. The SWNTs are seen forming large bundles and are at the surface of a polymer/surfactant matrix. The image shown on the right contains a large crack, which is a result of the drying process. The films studied were approximately 12.5  $\mu\text{m}$  thick.

The thermal time constant was obtained by applying a voltage pulse train to the bolometer through a load resistor using a function generator, and measuring the current response of the bolometer using a digital oscilloscope.<sup>12</sup> The thermal time constant ( $\tau$ ) was determined as the time it takes for the voltage on the bolometer to reach 63% of its maximum value.<sup>13</sup>

The current–voltage ( $I$ – $V$ ) characteristics were obtained at atmospheric pressure, at room temperature, and in both dark and illuminated conditions using a Keithley 617 electrometer while varying the applied voltage from 0.20 to 0.50 V, the voltage responsivity  $\mathcal{R}_V$  was calculated as a function of the applied voltage, using formula 2<sup>14–16</sup>

$$\mathcal{R}_V = \frac{\Delta V}{P_{inc}} \quad (2)$$

The illumination source was a tungsten-halogen lamp (Ocean Optics LS-1, 900 h) with a spectral emission range of 300 nm to 2  $\mu\text{m}$  and an emitted power of 0.48 mW over the whole spectral range. The peak power of this lamp is in the range of 700–950 nm, and drops off in strength after about 1850 nm.

Noise measurements were performed using a Hewlett-Packard HP3562A Dynamic Signal Analyzer, the noise of the system, and the total noise (system + noise of the device) were measured separately and then subtracted (in quadrature) to obtain the noise of the device.<sup>17</sup> In contrast to many other works, this method of measurement was chosen in place of using a chopper, which inherently adds a source of noise to the system and would limit the frequencies at which the studied bolometers could operate.

The detectivity  $D^*$  (“D-star”) was determined for the deposited film, as this figure of merit was first suggested by Jones<sup>18,19</sup> to normalize the performance of the detector to the square root of its area and measurement bandwidth. This can be expressed as eq 3

$$D^* = \frac{\mathcal{R}_V \sqrt{A_d}}{V_{noise}/\Delta f} \quad (3)$$

Where  $A_d$  is the area of the detector,  $\Delta f$  is the bandwidth of the bolometer/readout system,  $\mathcal{R}_V$  is the detector responsivity, and  $V_{noise}$  is the voltage noise.<sup>14,20</sup>

Noise equivalent power (NEP) is the incident detector radiation power for which the signal-to-noise ratio is equal to one for a specific wavelength. The NEP was calculated using formula 4

$$NEP = \frac{V_{noise}}{\mathcal{R}_V} \quad (4)$$

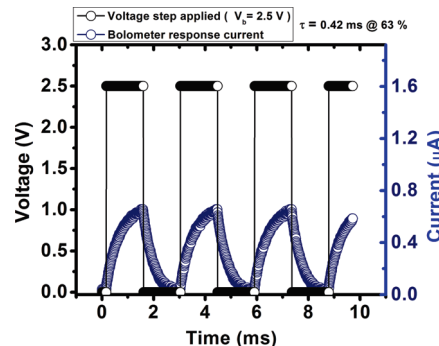


**Figure 2.** Thermal time constant obtained using a voltage pulse train. Response to this voltage pulse train confirms a bolometric response and not a photoconductive response.

### 3. RESULTS

Figure 1 shows a scanning electron micrograph of the SWNT films analyzed. Self-orientation of the SWNTs occurs during the deposition process, and likely occurs in two stages. During the initial evaporation, it has been observed that the droplet of ink does not change diameter but that the height is reduced. It is theorized that during this stage the SWNTs organize into very large bundle architectures. In the second stage of drying the droplet diameter changes quickly, withdrawing the edges toward the center. It is theorized that during this stage the self-orientation of the large bundle structures occurs. This self-orienting behavior is likely a result of the bundles crowding one another and forcing the ordering observed. The majority of the film is continuous, but several large cracks were observed that reveal arrays of suspended SWNTs. This has been shown in a previous work,<sup>10</sup> and may have an effect on the bolometric properties of these arrays. When a control sample with no self-orientation and no cracking was examined, the bolometric properties were good but significantly reduced (see the Supporting Information). The temperature coefficient of resistance of the SWNT film was obtained by heating with a Peltier thermoelectric device from 300 to 345 K, and measuring the resistance of the film in real time. The average TCR obtained was 2.94% K<sup>-1</sup> (standard deviation = 1.09% K<sup>-1</sup>) which is higher than the highest reported value for TCR ( $\sim 1.0\%$  K<sup>-1</sup>) in a carbon nanotube film at room temperature,<sup>2</sup> and even slightly better than the TCR of YBaCuO microbolometers (2.5% K<sup>-1</sup>).<sup>21</sup> This TCR value for our SWNTs films is in fact comparable to commercial vanadium oxide bolometers.<sup>2</sup> The standard deviation that we are reporting is considerable, but this value has not been reported in any of the previous works regarding carbon nanotube bolometers, and thus it can only be assumed that this deviation is inherent to such analysis. The negative TCR value is indicative of a semiconductor bolometer, and therefore it is likely that the semiconducting SWNTs are the most active carbon nanotubes in these bolometric devices.

The films were found to have an absorbance that increased steadily from 1300 nm to a peak absorbance at approximately 1800–1850 nm, and then dropping off to 2000 nm (see the Supporting Information). The conductivity of these films was approximately  $6.4 \times 10^{-5}$  S m<sup>-1</sup>.

Figure 2 shows the thermal response of the SWNT films which give an average thermal time constant of  $\tau = 420 \mu\text{s}$  measured at 63% pulse intensity.<sup>13</sup> This thermal response of the bolometers was evaluated with electrical testing that employed a voltage

Table 1. Comparison of Carbon Nanotube Bolometer Device Size and Bolometric Response Times<sup>a</sup>

publication	carbon nanotube	approximate device area (mm <sup>2</sup> )	magnitude of voltage response (%)	response time	absolute TCR at $\geq 298^\circ$ K (% K <sup>-1</sup> )	responsivity at room temperature/pressure (V/W)	detectivity (cm Hz <sup>1/2</sup> /W)
Itkis et al. <sup>2</sup> (2006)	SWNT	1.75	0–50	50 ms	1	~30	N/A
Aliev (2008) <sup>9</sup>	SWNT	1.48	0–50	<1 s	0.3	~150	N/A
Lu et al. <sup>24,3</sup> (2009, 2010)	SWNT	0.073	10–90	40–50 ms	0.17	N/A	$3.5 \times 10^5$
Lu et al. <sup>3</sup> (2010)	MWNT	0.073	10–90	1.0–2.5 ms	0.07	N/A	$3.3 \times 10^6$
Xiao et al. <sup>23</sup> (2011)	MWNT	10	N/A	4.4 ms	0.144	30	N/A
current work	SWNT	76	10–90	0.94 ms	2.94	230	$1.22 \times 10^8$

<sup>a</sup> The current work reports the some of the largest devices with perhaps the fastest bolometric response time reported to date. Those data that are not available are marked N/A.

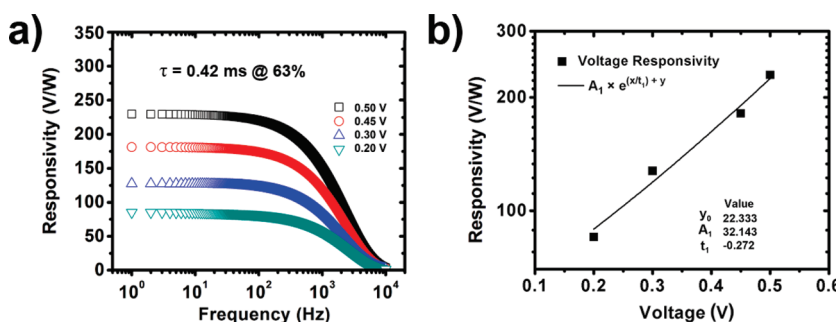
Figure 3. (a) Dependence of responsivity  $\mathcal{R}_V$  of SWNTs thin films on frequency, (b) maximum responsivity  $\mathcal{R}_V$  as a function of bias voltage.

Table 2. Thermoelectrical Parameters of SWNTs at Different Bias Voltages

SWCNTs	responsivity	NSD	detectivity	NEP (Watts)
	(V/W)	( $\mu$ V/Hz <sup>1/2</sup> )	(cm Hz <sup>1/2</sup> W <sup>-1</sup> )	
$V_{bias}$ (V)	@ 1.25 kHz	@ 1.25 kHz	@ 1.25 kHz	@ 1.25 kHz
0.20	50.40	1.21	$4.16 \times 10^7$	$24.00 \times 10^{-9}$
0.30	75.46	1.17	$6.45 \times 10^7$	$15.50 \times 10^{-9}$
0.45	107.30	1.12	$9.53 \times 10^7$	$10.50 \times 10^{-9}$
0.50	136.00	1.10	$1.220 \times 10^8$	$8.19 \times 10^{-9}$

pulse train, which is described in greater detail elsewhere.<sup>22</sup> The voltage responsivity ( $\mathcal{R}_V$ ) was calculated from the voltage response ( $\Delta_V = V_{IR} - V_{dark}$ , where  $V_{dark}$  is the dark voltage and  $V_{IR}$  is the voltage under illumination) at a fixed current, and dividing it by the incident power.<sup>14–16</sup> The bolometers reported in the current work have some of the fastest response times reported for carbon nanotube-based bolometers,<sup>2,3,23</sup> and yet they are also some of the largest bolometers that have been studied, with an active area of approximately 76 mm<sup>2</sup>. Generally, larger bolometers afford greater sensitivity, but slower response times. Previous works have shown similar response times as those shown in the current work, but with much smaller carbon nanotube bolometers, as is illustrated in Table 1.

Responsivity  $\mathcal{R}_V$  as a function of frequency was calculated from the thermal time constant.<sup>26</sup> Figure 3a shows a typical frequency response measurement, it can be seen that  $\mathcal{R}_V$  decreases with the frequency to a value of  $\mathcal{R}_V = 136$  V/W at  $\tau = 420$   $\mu$ s measured at 63% pulse intensity and a bias voltage of 0.50 V. It can be seen that the responsivity drops off at about 1 kHz, reaching 63% of the normalized response at 1.25 kHz, and for this

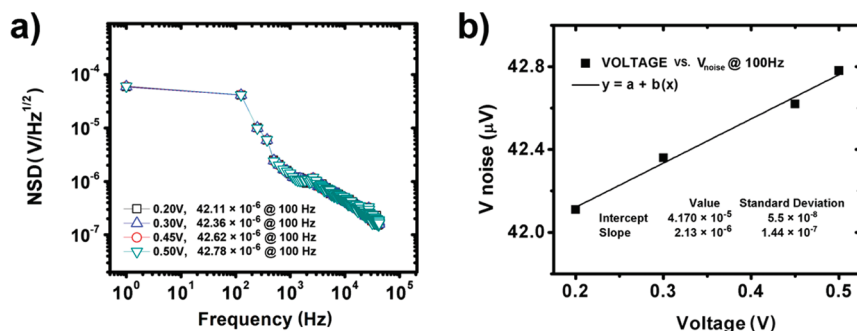
reason 1.25 kHz was chosen as the maximum reliable frequency for the devices studied. The responsivity  $\mathcal{R}_V$  of SWNT films as a function of the bias voltage is shown as Figure 3b.  $\mathcal{R}_V$  increases linearly with the bias voltage to a maximum value of  $\mathcal{R}_V = 230$  V/W at a bias voltage of 0.50 V, which is also higher than previously reported values of voltage responsivity for similar CNT films.<sup>9</sup> Table 2 shows the average  $\mathcal{R}_V$  value as a function of bias voltage, with a frequency of 1.25 kHz.

The noise characterization was performed under different DC voltages, measuring the spectral density of low frequency fluctuations using an HP3562A dynamic signal analyzer, which can measure noise power levels in a frequency range of 64  $\mu$ Hz to 100 kHz. The measurements were performed using the procedure described elsewhere.<sup>17,26</sup>

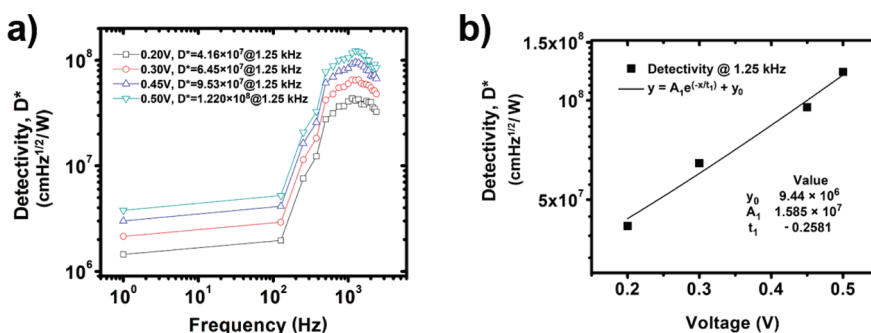
Figure 4 shows the voltage noise of the measured sample, these measurements follow the classical 1/f relationship given by  $NSD_V(f) \approx 1/f^\beta$ ,<sup>27</sup> where the  $\beta$  values ranged from  $\beta = 0.659$  for  $V_{bias} = 0.20$  V, to  $\beta = 0.663$  for  $V_{bias} = 0.50$  V. It is worth noting that these results are similar to those previously reported for plasma deposited a-Si:H semiconductor films with  $\beta$ -values ranging from 0.6 to 1.4.<sup>27</sup>

Figure 5 shows the detectivity plotted as a function of frequency for a bias voltage of 0.20–0.50 V. It can be seen from this graph that there is an increase in detectivity due to the fact that when the bias voltage increases, the voltage responsivity also increases, but at a higher rate than the voltage noise (eq 2). The maximum detectivity is seen at 1.25 kHz, and the values at each bias voltage are shown.

The detectivity of the devices reported here ( $1.22 \times 10^8$  cm Hz<sup>1/2</sup>/W) outperform any previously reported SWNT-based bolometer ( $3.5 \times 10^5$  cm Hz<sup>1/2</sup>/W,<sup>3</sup>), and even a previously reported MWNT-based bolometer ( $3.3 \times 10^6$  cm Hz<sup>1/2</sup>/W,<sup>3</sup>), but



**Figure 4.** (a) Noise spectral density  $NSD_V(f)$  for SWNT films as a function of frequency, with values at 100 Hz listed for each voltage tested. (b) Total noise voltage per unit bandwidth as a function of bias voltage.



**Figure 5.** (a) Detectivity  $D^*$  as a function of frequency, with values at 1.25 kHz listed for each voltage tested. (b) Detectivity per unit bandwidth as a function of bias voltage.

do not outperform state-of-the-art microbolometers based on a:  $Si_xGe_yB_z:H$  ( $3.4 \times 10^9$  cm Hz $^{1/2}$ /W<sup>28</sup>), but comparable to the detectivity of films of vanadium oxides ( $2 \times 10^8$  cm Hz $^{1/2}$ /W<sup>29</sup>). Recently it was reported that a SWNT thermopile showed a detectivity of  $2 \times 10^6$  cm Hz $^{1/2}$ /W, which is 2 orders of magnitude lower than the work presented here.<sup>30</sup> Table 1 provides a comparison of the present work with the results of prior studies, showing that although the devices used in the present work are the largest studied to date, they also are able to provide high responsivity at very high speed.

#### 4. CONCLUSIONS

In this work, films of horizontally aligned single-walled carbon nanotubes (SWNTs) were thermally and electrically characterized in order to assess their performance as bolometric materials. In the frequency range from 1 to 40 kHz the noise spectra had a  $1/f^\beta$  behavior with a  $\beta$  value varying from  $\beta \approx 0.659$  to  $\beta \approx 0.663$  depending on the bias voltage, this indicates a semiconductor-like noise behavior similar to the one reported for a-Si:H semiconductor films.<sup>25</sup>

The bolometric response times of the SWNT bolometers studied in the current work are some of the fastest reported to date, despite the fact that SWNTs typically yield slower devices than MWNTs.<sup>3</sup> The devices reported here are also significantly larger than previously studied CNT bolometers, affording greater sensitivity.

The values obtained for the voltage responsivity and detectivity at the optimal bias voltage of 0.50 V were  $\mathcal{R}_V = 230$  V/W and  $D^* = 1.220 \times 10^8$  cm Hz $^{1/2}$ /W, respectively. The value obtained for the voltage responsivity is significantly higher than

the maximum value of 150 V/W previously reported,<sup>9</sup> and suggests that dense networks of horizontally aligned SWNTs have potential as superior bolometric materials. Carbon-nanotube-based bolometers have a marked advantage over metallic bolometers in that they have been shown in the current work to be very low noise systems. Furthermore, it is possible to deposit these horizontally aligned nanotube arrays on a variety of substrates. Therefore the current work not only shows superior bolometric properties but also a more easily employed fabrication technique. The negative value for the TCR was indicative of semiconductor properties (reduced resistance at higher temperatures), which suggests that the semiconducting SWNTs were the most active carbon nanotubes in our devices. Because most commercially available SWNTs exist as a mixture of semiconducting and metallic nanotubes, an area for future improvement of these devices would possibly be the use of exclusively semiconducting nanotubes.

Future work will focus on increasing the alignment and density of the CNT films and on experimenting with a variety of carbon nanotube materials, such as multiwalled, functionalized, and doped carbon nanotubes, to determine the possible effect on bolometric properties. Additionally, the effect of the few large cracks that reveal large arrays of suspended SWNTs has not been evaluated, and further work will be required to elucidate the possible positive or negative effects.

#### ASSOCIATED CONTENT

**Supporting Information.** Additional SEM images regarding film orientation and absorbance are provided, along with an

additional set of thermal time constant measurements. This material is available free of charge via the Internet at <http://pubs.acs.org>.

## ■ AUTHOR INFORMATION

### Corresponding Author

\*E-mail: [javier.gonzalez@uaslp.mx](mailto:javier.gonzalez@uaslp.mx). Tel: +52 (444) 825-0183, ext 232. Fax: +52 (444) 825-0198.

### Author Contributions

<sup>†</sup>These authors contributed equally to this work.

## ■ ACKNOWLEDGMENT

The authors acknowledge support from CONACyT through Grant CB-2006-60349 and 48296, as well as financial support from the Coordinación para la Innovación y la Aplicación de la Ciencia y la Tecnología, CIACyT-UASLP. G.V. acknowledges the scholarship from CONACyT 182346 and acknowledges the support of Ismael Cosme B. (INAOE) for their help with the noise measurements.

## ■ REFERENCES

- (1) Kumar, R. T. R.; Karunagaran, B.; Mangalaraj, D.; Narayandass, S. K.; Manoravi, P.; Joseph, M.; Gopal, V. *Smart Mater. Struct.* **2003**, *12*, 188–192.
- (2) Itkis, M. E.; Borondics, F.; Yu, A.; Haddon, R. C. *Science* **2006**, *312*, 413–416.
- (3) Lu, R.; Li, Z.; Xu, G.; Wu, J. Z. *Appl. Phys. Lett.* **2009**, *94*, 163110.
- (4) Liu, C.; Bard, A. J.; Wudl, F.; Weitz, I.; Heath, J. R. *Electrochem. Solid-State Lett.* **1999**, *2*, 577–578.
- (5) Claye, A. S.; Fisher, J. E.; Huffman, C. B.; Rinzler, A. G.; Smalley, R. E. *Electrochem. Soc.* **2000**, *147*, 2845–2852.
- (6) Hone, J.; Llaguno, M. C.; Biercuk, M. J.; Johnson, A. T.; Batlogg, B.; Benes, Z.; Fisher, J. E. *Appl. Phys. A: Mater. Sci. Process.* **2002**, *74*, 339–343.
- (7) Baughman, R. H.; Cui, Ch.; Zakhidov, A. A.; Iqbal, Z.; Barisci, J. N.; Spinks, G. M.; Wallace, G. G.; Mazzoldi, A.; De Rossi, D.; Rinzler, A. G.; Jaschinski, O.; Roth, S.; Kertesz, M. *Science* **1999**, *284*, 1340–1344.
- (8) Lu, R.; Xu, G.; Wu, J. Z. *Appl. Phys. Lett.* **2008**, *93*, 213101.
- (9) Aliev, A. E. *Infrared Phys. Technol.* **2008**, *51*, 541–545.
- (10) Simmons, T. J.; Hashim, D.; Vajtai, R.; Ajayan, P. M. *J. Am. Chem. Soc.* **2007**, *129*, 10088–9.
- (11) Bravo-Sánchez, M.; Trevor, J. S.; Vidal, M. A. *Carbon* **2010**, *48*, 3531–3542.
- (12) Moreno, M. M. *Doctoral Thesis* **2008**, 69–73.
- (13) Monkman, G. J.; Taylor, P. M. *IEEE Trans. Rob. Autom.* **1993**, *9*, 313–318.
- (14) Liu, S. T.; Long, D. *Proc. IEEE* **1978**, *66*, 14–26.
- (15) Beerman, P. H. *IEEE Trans. Electron Devices* **1969**, *16*, 161–165.
- (16) Ciupa, R.; Rogalski, A. *Opto-Electron. Rev.* **1997**, *5*, 257–266.
- (17) González, F. J. *Rev. Mex. Fís.* **2006**, *52*, 550–554.
- (18) Jones R. C. *Advances in Electronics*; Academic Press: New York, 1952; Vol. , 5.
- (19) Jones, R. C. *Proc. IRE* **1959**, *47*, 1495–1502.
- (20) Hossain, A.; Rashid, H. M. *IEEE Trans. Ind. Appl.* **1991**, *27*, 824–829.
- (21) Mérel, P.; Kpetsu, J. B. A.; Koechlin, C.; Maine, S.; Haidar, R.; Pélouard, J. L.; Sarkissian, A.; Ionescu, M. I.; Sun, X.; Laou, P.; Paradis, S. *C.R. Phys.* **2010**, *11*, 375–380.
- (22) Sedky, S.; Fiorini, P.; Caymaxa, M.; Baert, C.; Hermans, L.; Mertens, R. *IEEE Electron Device Lett.* **1998**, *19*, 376–378.
- (23) Xiao, L.; Zhang, Y.; Wang, Y.; Liu, K.; Wang, Z.; Li, T.; Jiang, Z.; Shi, J.; Liu, L.; Li, Q. Q.; Zhao, Y.; Feng, Z.; Fan, S.; Jiang, K. *Nanotechnology* **2011**, *22* (025502), 7.
- (24) Lu, R.; Li, Z.; Xu, G.; Wu, J. Z. *Appl. Phys. Lett.* **2009**, *94* (163110), 3.
- (25) Kosarev, A.; Moreno, M.; Torres, A.; Rumyantsev, S.; Cosme, I. *Thin Solid Films* **2010**, *518*, 3310–3312.
- (26) González, F. J. *Microwave Opt. Technol. Lett.* **2000**, *26*, 291–293.
- (27) Johanson, R. E.; Guenes, M.; Kasap, S. O. *IEEE Proc. Circuits Devices Syst.* **2002**, *149*, 68–74.
- (28) Moreno, M.; Kosarev, A.; Torres, A.; Juarez, I. *J. Non-Cryst. Solids* **2008**, *354*, 2552–2555.
- (29) Chen, C.; Yi, X.; Zhao, X.; Xiong, B. *Sens. Actuators, A* **2001**, *90*, 212–214.
- (30) St-Antoine, B. C.; Ménard, D.; Martel, R. *Nano Lett.* **2011**, *11* (2), 609–613.